# VALIDATION OF SPALLATION MODELS FOR $p$+Al REACTIONS AT 180 MeV INCIDENT PROTON BEAM ENERGY

Sushil K. Sharma[†], B. Kamys

The Marian Smoluchowski Institute of Physics, Jagiellonian University
Reymonta 4, 30-059 Kraków, Poland

F. Goldenbaum, D. Filges

Institut fuer Kernphysik, Forschungszentrum Juelich, 52425 Juelich, Germany

*(Received June 17, 2014)*

Various observables measured at low beam energy of 180 MeV for proton induced reactions on $^{27}$Al targets have been compared with theoretical predictions of different spallation models. These models assume that the reactions proceed in two stages: the intranuclear cascade of nucleon–nucleon collisions followed by the de-excitation of equilibrated, excited remnants of the cascade. The calculations of the intranuclear cascade were performed by means of the INCL4.6 code, whereas the second stage of the reactions was realized using four different models: ABLA07, GEMINI++, GEM2, and SMM. It was found that the main properties of the experimental isobaric total production cross sections are reasonably well reproduced by all these spallation models. The shape of the energy averaged angular distributions of ejectiles with $A = 7$, 12, 16, 22, 24, and 25 was also well described by the models listed above, however the absolute magnitude of $A = 7$ and $A = 25$ data is strongly underestimated and overestimated, respectively. The theoretical energy spectra for $A = 7$, $A = 16$, and $A = 22$ are very similar for all the models and reproduce well the data for heavier ejectiles, whereas the $A = 7$ data deviate from the model cross sections for energies smaller than $\approx$ 10 MeV what may indicate the presence of a reaction mechanism not included in the spallation models. The following ranking of the four used models — all of them being coupled to the very same INCL4.6 INC model — was determined using the statistical $H$-test in a quantitative analysis: (1) GEMINI++, (2) SMM, (3) ABLA07, and (4) GEM2.

DOI:10.5506/APhysPolB.45.1963
PACS numbers: 25.40.Sc, 25.40.Kv, 25.40.–h

[†] Corresponding author: sushil.sharma@uj.edu.pl

## 1. Introduction

Proton induced reactions play an important role in many fields of science and technology, *e.g.*, in astrophysics, accelerator driven systems, neutron spallation sources, nuclear waste transmutation, nuclear synthesis, radioactive ion beams, *etc.* Thus, the knowledge of cross sections and reaction mechanism characterizing these processes is indispensable. It is obvious that the experimental determination of cross sections for all possible targets in a broad range of proton energies (from tens of MeV to several GeV) and for vast amount of product nuclides is practically not possible because of technical reasons (*e.g.* short living unstable target nuclei) as well as of time constraints for necessary experiments. Therefore, one has to rely on theoretical models of the reaction mechanism to interpolate and extrapolate the measured cross sections to energies and nuclear systems which are difficult to be investigated experimentally. Many models have been proposed for this purpose [1]. They differ by physical assumptions as well as by numerical methods used for the evaluation of observables what influences their range of applicability.

It is generally believed that the protons which are represented by wave packets of dimensions smaller than about 1 fm, *i.e.* protons of GeV energies induce spallation reactions which proceed in two steps. The first step is provided by the intranuclear cascade model of two-body nucleon–nucleon collisions since the average distance between nucleons in the nucleus is larger than the dimensions of the impinging proton. Several nucleons and eventually pions are emitted during this first stage of the reaction leaving behind the residuum of the target in an excited state. The second stage of the reaction consists in the de-excitation of the remnant nucleus which, in most of the models, is assumed to be equilibrated. There are also models which add the pre-equilibrium stage between the intranuclear cascade and the process of emission from the equilibrated residua of the cascade.

To use such models as a reliable tool to describe the reaction mechanism, it is very important to find the range of applicability of the specific reaction models. In references [2, 3], a comparison of calculations performed with seventeen different models or different combinations of intranuclear cascade and de-excitation models with selected set of data from proton induced reactions on different targets with the focus on Pb and Fe is presented. The emission channels cover neutrons, light charged particles (LCPs), *i.e.* $p$, $d$, $t$, $^3$He and $^4$He, and target residua for proton beam energies ranging from 20 MeV to 3 GeV. It has been found that the intranuclear cascade plus de-excitation models give reasonable predictions even at energies smaller than 150 MeV, where such models from the basic physics assumptions are not expected to work well. It was also concluded that there is no clear advantage of introducing the intermediate preequilibrium stage.

As concerns neutron data, practically all models were in comparable, reasonable agreement. The combinations of intranuclear cascade model INCL4.5 [4] with the following three models: SMM [5–8], ABLA07 [9], and GEMINI++ [10, 11] were slightly superior in comparison to other models.

The calculations performed for LCPs using the same models were often found to agree rather well with some sets of data and disagree with some other sets, making it difficult to draw categorical conclusions on the best model. It was emphasized, that a specific process (coalescence for example) is necessary to reproduce high-energy tails in the spectra of LCPs. It has been previously shown [12] that the INCL4.5 model of the intranuclear cascade which takes into consideration possibility of the coalescence of nucleons into composite light charged particles predicts well helium and tritium cross sections over a wide incident energy range when coupled with the ABLA07 model describing the emission of these particles from the second stage of the reaction.

Conclusions concerning the residue production have been found to be the most difficult ones since the rating depends on the choice of mass and charge distributions or isotopic distributions to the analysis. A good description of a mass or charge distribution may be accompanied by deficits in the description of isotope distributions. Reproduction of the isotope distributions was generally worse than that for mass and charge distributions. The rating of the agreement between theory and experiment for isotope distributions favourized clearly the combination of INCL4.5 + ABLA07 models [2, 3].

In the last years, the new version INCL4.6 of the original INCL model has been developed to allow for coalescence of the nucleons from the intranuclear cascade into complex particles heavier than $^4$He. It was shown by Boudard *et al.* [13] that this new version of the intranuclear cascade code coupled to the program ABLA07 gives a generally good agreement for a large set of observables (total reaction cross sections, neutron, proton, pion, and composite double-differential cross sections, neutron multiplicities, residue mass and charge distributions, and residue recoil velocity distributions) for proton induced reactions in the 200 MeV to 2 GeV range. Below 200 MeV and down to a few tens of MeV, the total reaction cross section is well reproduced for a broad range of targets, whereas the description of differential cross sections is still reasonable when using Fe, Ni, Au, and Pb targets.

The aim of the present work is to investigate the accuracy of the data reproduction by the INCL4.6 model [13] coupled to four different models describing the second stage of the reaction: ABLA07 [9], GEMINI++ [10, 11], GEM2 [14, 15] and SMM [5–8] for a light target at incident proton beam energies below 200 MeV. The aluminium target was selected for this purpose because the most complete inclusive data for $p$+Al collisions were obtained by Kwiatkowski *et al.* [16] at proton beam energy of 180 MeV. They consist

of isobaric integral cross sections $\sigma(A) \equiv d\sigma/dA$ for products with mass number $A = 6$–$25$, isobaric angular distributions $d^2\sigma/d\Omega dA$ for $A = 7$, 12, 16, 22, 24, and 24, as well as isobaric energy spectra $d^3\sigma/d\Omega dEdA$ for $A = 7$, $A = 16$, and $A = 22$. To our knowledge, in the literature there are neither reported exclusive measurements of the reactions in $p$+Al system at 180 MeV nor inclusive isotopic data for these reactions.

The data of Kwiatkowski *et al.* [16] were recently used by Sabra *et al.* [17] for the validation of four different models of proton induced reactions on an Al target. There were the following models: Binary Cascade Model (BIC) [18], the Cascade Exciton Model (CEM3.02A) [19] which uses the Generalized Evaporation Model (GEM) [14] in the evaporation stage, the JAEA Quantum Molecular Dynamics (JQMD) model [20] implemented, along with the Generalized Evaporation Model (GEM), in the Particle and Heavy-Ion Transport code (PHITS) version 2.1.4 [21], referred to in this work as PHITS, as well as the Statistical Model with a Final State Interaction (SMFSI) [22, 23]. This enabled us to compare the quality of the description of the same data by INCL4.6 model coupled to ABLA07, GEMINI++, GEM2, and SMM with that obtained by the models used by Sabra *et al.* [17] which treat the reaction mechanism with noticeably different parametrization. As it was mentioned above, the models which we selected for the comparison with the low energy $p$+Al data were found to be superior to other models in the analysis of higher energy data obtained for heavy targets [3]. It is, therefore, important to know whether this is also true for a light target and low energy data.

In Sec. 2 the analysis of the isobaric production cross sections $d\sigma/dA$ is presented for ejectiles with mass number $A = 6$–$25$ measured by Kwiatkowski *et al.* [16] at proton beam energy equal to 180 MeV. The next section is devoted to the analysis of angular distributions $d^2\sigma/d\Omega dA$ and spectra $d^3\sigma/d\Omega dEdA$ of these ejectiles. Results are discussed and summarized in the last section.

## 2. Analysis of isobaric $d\sigma/dA$ cross sections for $p$+Al collisions at proton energy 180 MeV

The isobaric cross section $d\sigma/dA \equiv \sigma(A)$ for products of $p$+Al collisions with mass number $A$ in the range from 6 to 25 were evaluated in the frame of a two-step model. The first step of the reaction, *i.e.* cascade of nucleon–nucleon collisions was described by means of the INCL4.6 model, which besides the emission of nucleons allows also for the coalescence of nucleons into complex fragments up to mass number $A_F \leq 8$ [13]. The second step of the reaction, *i.e.* the emission of particles from excited residuum of the intranuclear cascade was described by four different models: ABLA07,

GEMINI++, GEM2, and SMM. The theoretical cross sections were evaluated only for particles with kinetic energy larger than 0.05 MeV/$u$ since in the experiment of Kwiatkowski *et al.* [16] only such products of the reaction were detected.

As can be seen in Fig. 1, the histograms reproduce characteristic properties of the isobaric cross sections: *(i)* the cross sections increase on average with the mass number, and *(ii)* the cross sections for fragments with the mass number in the neighbourhood of $A = 12$, $A = 16$, and $A = 20$ are larger than those for other fragments. This is an expected effect due to a stronger binding of "alpha-nuclei". On the other hand, the sum of experimental cross sections seems to be larger than the sum of the theoretical cross sections for each of the models. Such a disagreement may lead to the conjecture that there is some systematic error of the absolute normalization of the experimental cross sections since the model cross sections are evaluated

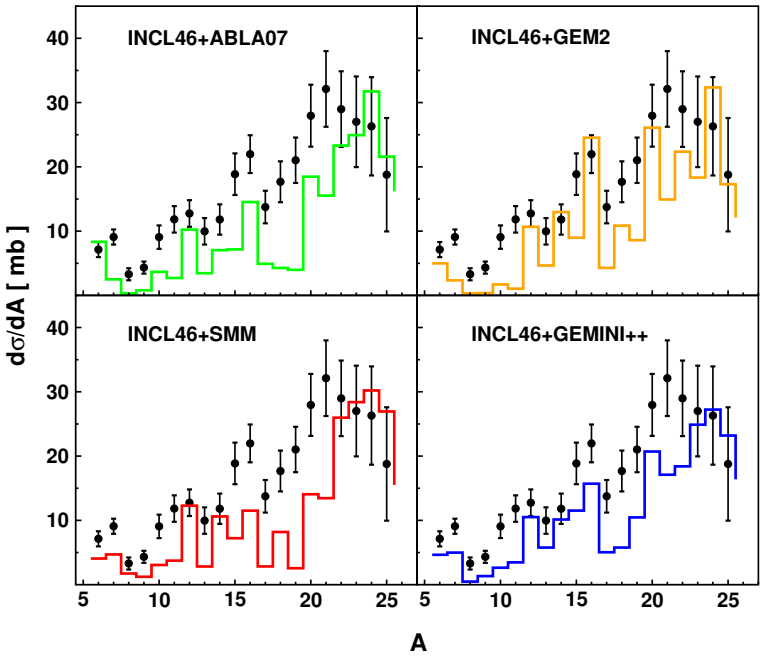


Fig. 1. Isobaric cross sections are presented as a function of fragment mass number $A$ for proton induced reactions on Al at 180 MeV. Experimental data (•) of Kwiatkowski *et al.* [16] are compared with theoretical calculations (histograms) performed by means of the intranuclear cascade INCL4.6 code coupled to ABLA07 (upper left panel), SMM (lower left panel), GEMINI++ (lower right panel), and GEM2 (upper right panel) codes used for description of the de-excitation of the residua of the intranuclear cascade.

without free parameters. The authors of Ref. [16] estimated the value of the total reaction cross section for these data to be between 370 mb (assuming that all fragments with $6 \leq A \leq 9$ have heavy partners) and 394 mb (assuming that all fragments with $A > 6$ have no heavy partners). They claim that this values are consistent within experimental uncertainties (10–15%) with the reaction cross section of 410 mb extracted from the analysis of the elastic scattering data. However, it should be taken into consideration that the not measured light products of the $p$+Al collisions with mass $A < 6$ can be produced with relatively large cross sections (especially nucleons and alpha-particles). Thus the total cross section extracted from the products with $6 \leq A \leq 25$ should be significantly smaller than that obtained from the elastic scattering. Indeed, the authors of Ref. [16] found that the semiempirical estimation [24] of the total cross section for measured data gives value of the total cross section equal to 326 mb, *i.e.* equal to 82–88% of their experimental value. This uncertainty of the absolute normalization of the experimental data was taken into account during searching for the best theoretical model as it is described below.

Many statistical tests were proposed in the literature to establish the ranking of the data description by different theoretical models [25]. In the present study, the $H$-test defined by the following equation has been applied

$$H \equiv \left[ \frac{1}{N} \sum_{i=1}^{N} \left( \frac{\sigma_i^{\mathrm{exp}} - \sigma_i^{\mathrm{cal}}}{\Delta\sigma_i^{\mathrm{exp}}} \right)^2 \right]^{1/2}, \tag{1}$$

where $\sigma_i^{\mathrm{exp}}$, $\Delta\sigma_i^{\mathrm{exp}}$, and $\sigma_i^{\mathrm{cal}}$ have the meaning of the $i^{\mathrm{th}}$ experimental cross section, its error and the corresponding model ("calculated") cross section, respectively. This test has several appealing properties: *(i)* its value is proportional to the distance between two points in the $N$-dimensional space $|\vec{\sigma}^{\,\mathrm{exp}} - \vec{\sigma}^{\,\mathrm{cal}}|$ calculated in units of the statistical error of the cross section $\Delta\sigma_i^{\mathrm{exp}}$, *(ii)* in the case when the experimental cross section may be treated as the Gaussian variable with the expectation value equal to the model cross section, *i.e.*, for the perfect agreement of the model and experimental cross sections, the probability distribution function of the $H$-test may be written in the analytic form (Eq. (2)), *(iii)* this distribution depends then only on the number $N$ of the analyzed cross sections and has known expectation value and standard deviation (Eqs. (3) and (4)) [26]

$$h(H) = \frac{N^{\frac{N}{2}}}{2^{\frac{N}{2}-1}\Gamma\left(\frac{N}{2}\right)} \exp\left(-\frac{NH^2}{2}\right) H^{N-1}, \tag{2}$$

$$E(H) = \sqrt{\frac{2}{N}} \frac{\Gamma\left(\frac{N+1}{2}\right)}{\Gamma\left(\frac{N}{2}\right)}, \tag{3}$$

$$\sigma(H) = \sqrt{1 - E\,(H)^2}\,. \tag{4}$$

Since the distribution of the $H$-test is similar to the normal distribution, the standardized $H$-test ($z(H) \equiv (H - E(H))/\sigma(H)$) can be treated as the standard normal variable. Thus, it is easy to test the hypothesis of the perfect agreement of the model and the experimental cross sections as well as to interpret the value of the $z(H)$ variable. The estimates of the mean value $E(H)$ and the standard deviation $\sigma(H)$ of the $H$-test for the analyzed set of isobaric cross sections $\sigma(A)$ are equal to 0,9930 and 0,1614, respectively.

In the present analysis, we would like *(i)* to determine the ranking of the quality of the data description by four used theoretical models assuming that the experimental data are properly normalized, and *(ii)* to check whether the uncertainty of the absolute normalization of the cross sections influences the ranking of the models.

• *ad (i)* The data and histograms presented in Fig. 1 were used to calculate the values of the $H$-test as well as the standardized values $z(H)$ of this test for four models, *i.e.* for INCL4.6 coupled with ABLA07, GEMINI++, GEM2, and SMM. These values are listed in first four rows of Table I. The $H$-test (the second column of the table) has the smallest value for GEMINI++, it is almost the same for SMM and GEM2 — larger by about 25% than that for GEMINI++, and $H$-test for ABLA07 is the largest — about 7% larger than for SMM and GEM2. The standardized test $z(H)$ (the third column of the table) changes from 9.5 for GEMINI++ to 12.8 for ABLA07, *i.e.* it deviates more than 9 standard deviations from zero value expected for the perfect agreement of the model and experimental cross sections. Such a result cannot be treated as the indication of good reproduction of the data, however, it determines unambiguously the ranking of the models: (1) GEMINI++, (2–4) SMM, GEM2, and ABLA07.

• *ad (ii)* The possibility of changing the absolute normalization of the cross sections can be taken into consideration in evaluation of the $H$-test by introducing the scaling factor which multiplies all the experimental cross sections and their statistical errors. It was found that multiplication of the data and errors by scaling factor changes smoothly the values of the $H$-test. This is illustrated by Fig. 2. The inspection of this figure leads to the conclusion that the reproduction of the data by GEMINI++ is the best for all reasonable values of the scaling factor (from 0.5 to 1.5). Thus, the GEMINI++ histogram is also the best for the original data (*i.e.* with the scaling factor equal to 1), whereas all other models reproduce the original data with almost the same quality.

TABLE I

In the first column the name of the model is depicted. The second column presents the value of the $H$-test and the third column the value of $z(H)$, *i.e.* the standardized $H$-test. In the fourth column the scaling factor $\mathrm{SF}(H_{\min})$ is given for which the minimal value $H_{\min}$ of the $H$-test was obtained, in the fifth column the minimal value $H_{\min}$ is listed, and in the sixth column its standardized value $z(H_{\min})$. The last column presents the relative improvement of the $H$-test (in percent) due to adjustment of the scaling factor.

| Model | $H$ | $z(H)$ | $\mathrm{SF}(H_{\min})$ | $H_{\min}$ | $z(H_{\min})$ | $\Delta z/z(H)\%$ |
|---|---|---|---|---|---|---|
| GEMINI++ | 2.52 | 9.5 | 0.65 | 1.81 | 5.1 | 46 |
| GEM2 | 2.90 | 11.8 | 0.78 | 2.72 | 10.7 | 10 |
| SMM | 2.94 | 12.1 | 0.66 | 2.45 | 9.0 | 25 |
| ABLA07 | 3.06 | 12.8 | 0.69 | 2.70 | 10.6 | 17 |
| PHITS | 2.55 | 9.7 | 0.87 | 2.47 | 9.2 | 5 |
| CEM | 3.33 | 14.5 | 0.75 | 3.15 | 13.4 | 8 |
| BIC | 3.47 | 15.4 | 0.96 | 3.47 | 15.3 | 0 |
| SMFSI | 4.54 | 21.9 | 1.64 | 3.84 | 17.6 | 20 |

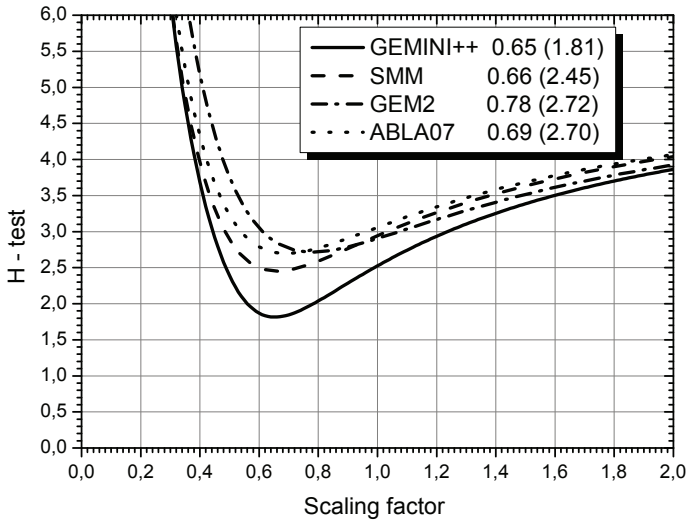


Fig. 2. The dependence of the $H$-test calculated for isobaric cross sections $d\sigma/dA$ of Kwiatkowski *et al.* [16] on the scaling factor used to multiply the experimental cross sections and their errors. Different lines correspond to appropriate models written in the legend of the figure. The first number written at the name of the model represents the value of the scaling factor at which the $H$-test has the minimum and the number in parenthesis depicts a $H_{\min}$ value.

The values of the $H$-test and the standardized $z(H)$ test for the best-fit scaling factor (depicted in the fourth column of Table I which is denoted by the title "SF") are listed in the fifth and the sixth columns of this table. The relative improvement of the $H$-test for the data scaled by the best-fit scaling factor in respect to the $H$-test evaluated for the original data is shown in the last column of the table. As can be seen, the improvement is substantial for GEMINI++ (46%), smaller for SMM (25%), and significantly smaller, *i.e.* 10% and 17% for GEM2 and ABLA07, respectively. This indicates that the shape of the histogram evaluated by GEMINI++ resembles better the shape of the experimental dependence of the isobaric cross section on the mass number of the reaction products than the other models, especially GEM2 and ABLA07. Furthermore, it is evident that the ranking of the models does not change by introducing reasonable values of the scaling factor, however, the differences between the models become more evident for the best-fit scaling factors.

It is worth mentioning that the best-fit scaling factor has a very similar value (0.65–0.78) for all four models. This value is substantially smaller than unity what is in accord with the hypothesis of systematic overestimation of the absolute values of the cross sections in the experiment of Kwiatkowski *et al.* [16] discussed above.

Due to the fact that the same isobaric cross sections of Kwiatkowski *et al.* [16] were recently analyzed by Sabra *et al.* [17] using four different models of the reaction, it was possible to repeat our analysis for these additional four models. Figure 3 of Ref. [17] shows that the qualitative properties of the theoretical histograms evaluated by means of their four models are quite similar to the properties of those which were obtained in our analysis. Thus, the ranking of all eight models can be done using the same quantitative $H$-test.

The values of the $H$-test and its standardized version — $z(H)$ for the models used by Sabra *et al.* are listed in the last four rows of Table I and the dependence of the $H$-test on the scaling factor of the data is presented in Fig. 3.

It turned out for the original data of Kwiatkowski *et al.* (*i.e.* for the scaling factor equal to unity), that among the four models used by Sabra *et al.*, the PHITS model produced almost exactly as good values of the $H$-test as GEMINI++ which is the best in our analysis. All other models applied by Sabra *et al.*, *i.e.*, CEM, BIC, and SMFSI resulted in poorer $H$-test values than all models used in the present analysis. This means that the ranking of the model description of the original (not scaled) isobaric cross sections may be written as follows: (1–2) GEMINI++, PHITS, (3–5) GEM2, SMM, ABLA07, (6) CEM, (7) BIC, (8) SMFSI.

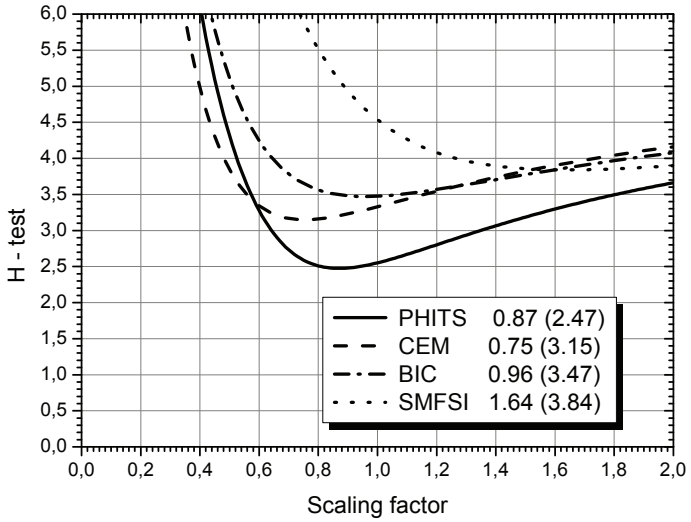


Fig. 3. The same as Fig. 2 but for four models applied by Sabra *et al.* [17].

The situation changed when the analysis was done for renormalized data. The dependence of the $H$-test on the scaling factor is different for models used by Sabra *et al.* and for those used in our analysis, *cf.* Figs. 2 and 3. The $H$-test values for models used in the present paper decreased significantly with changing the scaling factor from unity to the best-fit values, whereas the $H$-test values for models applied by Sabra *et al.* were almost independent of the normalization of the experimental data. Due to this, the ranking of the $H$-test for best-fit scaling factor is different than for the original data. Looking in Table I, the following ranking may be proposed: (1) GEMINI++, (2–3) SMM, PHITS, (4–5) ABLA07, GEM2, (6) CEM, (7) BIC, and (8) SMFSI.

## 3. Analysis of angular $d^2\sigma/d\Omega dA$ and energy $d^3\sigma/d\Omega dEdA$ distributions for $p$+Al collisions at proton energy 180 MeV

The energy integrated isobaric angular distributions $d^2\sigma/d\Omega dA$ measured by Kwiatkowski *et al.* [16] are presented in Fig. 4 as full dots for six values of the mass number of the emitted fragments: $A = 7$, 12, 16, 22, 24 and 25. Predictions of the INCL4.6 model coupled to four different models used for the description of the second stage of the reaction: ABLA07, GEMINI++, GEM2, and SMM are shown as lines. It is evident that all the models reproduce well the shape of angular distributions, however, this is not the case for the magnitude of the cross sections. The disagreement of the absolute values of the cross sections is especially pronounced for the $A = 7$ data which are strongly underestimated and for the $A = 25$ data which are significantly overestimated by all the models.

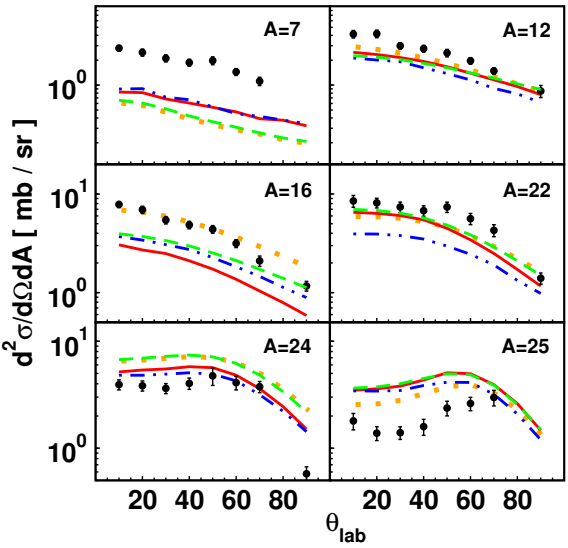


Fig. 4. (Color online) The energy integrated angular distributions for emitted fragments $A = 7$, 12, 16, 22, 24 and 25. Experimental data (•) were taken from Ref. [16]. Theoretical calculations were performed using INCL4.6 coupled with ABLA07 (dashed/green line), SMM (solid/red line), GEMINI++ (dot-dashed/blue line), and GEM2 (dotted/orange line).

To obtain a ranking of the description of angular distributions by different models, some quantitative measure has to be applied. For this purpose, the $H$-test values have been calculated for all ejectiles using the models listed above. All calculations were done for original normalization of the data. These values are collected in Table II for all ejectiles and models. The first four rows of the table contain $H$-values for models used in the present study, whereas the following four rows correspond to models applied by Sabra *et al.* [17]. As can be seen, $H$-values vary randomly from one to another model for the same ejectile as well as from one ejectile to another for the same model. Thus, only the averaged over all ejectiles $H$-test can serve as a reasonable estimate of the quality of reproduction of the data by the models. The averaged $H$-test values are listed in the last column of Table II. The best description of the energy averaged isobaric angular distributions $d^2\sigma/d\Omega dA$ was achieved by GEMINI++, whereas that of the SMM model is slightly poorer. Calculations performed by means of ABLA07 and GEM2 produce almost exactly equivalent description of the data but it is significantly worse than that provided by GEMINI++ and SMM. Thus the following ranking of the models may be proposed: (1) GEMINI++, (2) SMM, (3–4) ABLA07, GEM2.

TABLE II

Values of the $H$-test evaluated for the energy averaged isobaric angular distributions within different theoretical models (rows) for ejectiles with mass number $A = 7$, 12, 16, 22, 24, and 25 (columns). In the first column the name of the model is depicted, whereas in the last column the $H$-test averaged over all studied fragments is listed. The $H$-test for $A = 7$ and for the BIC model is not listed because the appropriate calculations were not shown in Ref. [17].

| Model | Mass number $A$ of the ejectile | | | | | | Mean |
|---|---|---|---|---|---|---|---|
| | 7 | 12 | 16 | 22 | 24 | 25 | $H$-test |
| GEMINI++ | 6.95 | 2.11 | 3.66 | 6.79 | 14.85 | 11.52 | 7.65 |
| SMM | 7.14 | 0.84 | 1.15 | 15.95 | 18.01 | 15.26 | 9.73 |
| ABLA07 | 8.05 | 1.28 | 5.10 | 17.98 | 26.32 | 15.17 | 12.32 |
| GEM2 | 8.24 | 0.97 | 16.23 | 15.27 | 25.68 | 10.15 | 12.76 |
| SMFSI | 0.70 | 3.84 | 14.57 | 17.24 | 5.86 | 1.06 | 7.21 |
| PHITS | 8.30 | 1.73 | 12.09 | 14.62 | 25.12 | 19.60 | 13.58 |
| CEM | 9.62 | 5.16 | 6.84 | 13.63 | 34.24 | 24.31 | 15.63 |
| BIC | — | 2.70 | 12.10 | 19.01 | 29.02 | 29.32 | 18.43 |

As concerns the models used by Sabra *et al.* [17] in their analysis of the same data, the SMFSI is clearly superior to other models in reproduction of the angular distributions. The next ranks belong to PHITS, CEM, and BIC. It is interesting to note that this is quite opposite situation to that which appeared for analysis of the total isobaric cross sections discussed in Sec. 2 where the SMFSI model was the worst.

Ranking of all the models listed in Table II with respect of the quality of the description of angular distributions is as follows: (1–2) SMFSI, GEMINI++, (3) SMM, (4–5) ABLA07, GEM2, (6) PHITS, (7) CEM, and (8) BIC.

It is important to check whether other observables confirm the rankings obtained from the analysis of total isobaric cross sections and of the energy integrated angular distributions. The experiment of Kwiatkowski *et al.* [16] provided such exclusive data, namely, the energy spectra of the isobaric cross sections — $d^3\sigma/d\Omega dAdE$ at several scattering angles for $A = 7$, $A = 16$, and $A = 22$. Unfortunately, these spectra are presented without errors in Ref. [16]. Therefore, the quantitative analysis using the $H$-test cannot be performed. However, the agreement of the theoretical and experimental spectra may be judged using Fig. 5 where predictions of four models used in the present investigations are shown together with the data.

The agreement of the models among themselves and with the data is the best for products with $A = 22$ (the lowest part of Fig. 5). This agreement is poorer for $A = 16$ (the middle part of Fig. 5). In particular, the

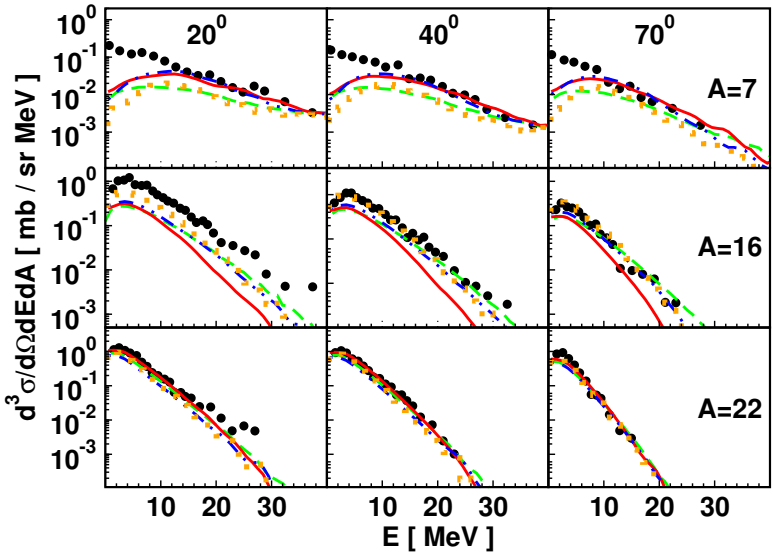


Fig. 5. (Color online) The energy spectra of double differential cross sections $d^2\sigma/d\Omega dE$ for ejectiles with $A = 7$, 16 and 22 at three different angles 20°, 40° and 70°. Experimental data (•) were taken from Ref. [16]. Theoretical calculations were performed using INCL4.6 coupled with ABLA07 (dashed/green line), SMM (solid/red line), GEMINI++ (dot-dashed/blue line), and GEM2 (dotted/orange line).

spectra evaluated with the SMM model have a different shape than for the other models and their absolute values are significantly smaller. The worst reproduction of the spectra is present for $A = 7$ (the upper part of Fig. 5). Admittedly, the shape of theoretical spectra is almost the same for all models (ABLA07, GEM2, GEMINI++, and SMM) but it does not agree with the shape of experimental spectra for energies smaller than about 10 MeV. At very small energies, the data are even one order of magnitude larger than the theoretical cross sections. Such an effect seems to indicate that the reaction mechanism responsible for emission of $A = 7$ ejectiles with very small energies is different from that proposed by the considered models.

In summary, all four models produce similar spectra which reproduce the experimental data with moderate success. None of the models seems to be evidently superior to others.

## 4. Summary and discussion

In the present paper calculations in the frame of different spallation models have been performed for $p$+Al collisions at proton beam energy of 180 MeV. An extensive set of data used for this analysis consisted of the

total isobaric cross sections $\sigma(A)$, the energy averaged angular distributions $d\sigma/d\Omega$ for mass number from $A = 6$ to $A = 25$, and the energy spectra $d^2\sigma/d\Omega dE$ for $A = 7$, $A = 16$, and $A = 22$ at three scattering angles (20, 40, and 70 degrees), measured by Kwiatkowski *et al.* [16].

It was found that the total isobaric cross sections were well reproduced by all models applied in the analysis, *i.e.* INCL4.6 cascade model coupled to ABLA07, GEM2, GEMINI++, and SMM models. The general trend of the mass number dependence as well as characteristic increase of the production of nuclides with mass number $A = 12$, 16, and 20 were reproduced. To validate the theoretical models quantitatively, the $H$-test (Eq. (1)) has been applied. It turned out that the $H$-test leads to the following ranking of the quality of the model description of the data: (1) GEMINI++, (2–3) SMM, GEM2, (4) ABLA07. Due to the fact that a similar analysis has been recently performed by Sabra *et al.* [17] for the same set of the total isobaric cross sections with four other spallation models, it was possible to extend the present ranking to these four models. The following ranking has been obtained: (1–2) GEMINI++, PHITS (3–5) GEM2, SMM, ABLA07, (6) CEM, (7) BIC, and (8) SMFSI.

In view of a possible inaccuracy of the absolute normalization of the isobaric data, the method of quantitative ranking of the models has been proposed. It consists in looking for the minimum of the $H$-test as a function of a scaling factor which multiplies both, the cross sections and their errors. It was found that the introduction of this additional degree of freedom almost does not modify the ranking made for the original normalization of the data, however, the differences between models become more evident for the best-fit scaling factors.

The quality of the description of the energy integrated angular distributions of isobaric cross sections $d^2\sigma/d\Omega dA$ led to a different ranking than that for the total cross sections, namely: (1–2) SMFSI, GEMINI++, (3) SMM, (4–5) ABLA07, GEM2, (6) PHITS, (7) CEM, and (8) BIC.

A comparison of the two rankings presented above shows that there are quite large differences for ranks of PHITS and SMFSI models in both rankings. It, therefore, seems to be reasonable to use the average of ranks from two rankings to obtain a final ranking. The individual ranks and the final ranking are presented in Table III.

The further analysis of the energy spectra of isobaric cross sections $d^2\sigma/d\Omega dE$ for $A = 7$, $A = 16$, and $A = 22$ could be done only qualitatively because the errors of these cross sections were not presented in the publication of Kwiatkowski *et al.* [16]. It was found that the shape of the theoretical spectra produced by all four models (GEMINI++, SMM, ABLA07, and GEM2) is almost the same for all ejectiles. It reproduces the experimental spectra for $A = 16$ and $A = 22$ but the theoretical cross sections

are significantly smaller than the experimental ones for $A = 7$ at energies smaller that $\approx 10$ MeV. This seems to indicate that the reaction mechanism for the production of these ejectiles is not contained in the spallation models.

TABLE III

The ranks of all eight models of the second stage of the spallation reactions. In the second and third column of the table, the ranks $r_1$ of the models obtained from the analysis of the total isobaric cross sections and $r_2$ of the energy averaged angular distributions from Ref. [16] are depicted, respectively. The tied ranks are shown when two models were equally well reproducing the data. The average of the ranks from these two columns are listed in the fourth column and the resulting final ranks are given in the fifth column.

| Model | $r_1$ | $r_2$ | $0.5(r_1 + r_2)$ | Final ranks |
|---|---|---|---|---|
| GEMINI++ | 1.5 | 1.5 | 1.5 | 1 |
| SMM | 4 | 3 | 3.5 | 2 |
| PHITS | 1.5 | 6 | 3.75 | 3 |
| ABLA07 | 4 | 4 | 4 | 4 |
| GEM2 | 4 | 5 | 4.5 | 5 |
| SMFSI | 8 | 1.5 | 4.75 | 6 |
| CEM | 6 | 7 | 6.5 | 7 |
| BCI | 7 | 8 | 7.5 | 8 |

We thank the code developers and authors A. Boudard, J. Cugnon, J.C. David, S. Leray and D. Mancusi for providing us the latest version of their Liege intranuclear cascade code INCL4.6. We are also grateful to A. Kelić-Heil for the improved version of ABLA07. One of us (S.K.S.) acknowledges gratefully the support by the Foundation for Polish Science — MPD program, co-financed by the European Union within the European Regional Development Fund.

## REFERENCES

[1] D. Filges *et al.*, Joint ICTP-IAEA Advanced Workshop on Model Codes for Spallation Reactions, IAEA INDC (NDS)-0530 (IAEA Publications, Vienna, 2008); D. Filges, F. Goldenbaum, *Handbook of Spallation Research*, 2009 Wiley-VCH Verlag, GmbH, Weinheim, Germany, ISBN-978-3-527-40714-9.

[2] J.-C. David *et al.*, *Prog. Nucl. Sci. Technol.* **2**, 942 (2011).

[3] S. Leray *et al.*, *J. Korean Phys. Soc.* **59**, 791 (2011).

[4] A. Boudard *et al.* (Eds.), Proceedings of the Joint ICTP-IAEA Advanced Workshop on Model Codes for Spallation Reactions, ICTP Trieste, Italy, 4–8 February, 2008, IAEA INDC(NDS)-530, Vienna, August 2008, p. 29, available from: `http://www-nds.iaea.org/reports-new/indc-reports/indc-nds/indcnds-0530.pdf`

[5] A.S. Botvina, A.S. Iljinov, I.N. Mishustin, *Sov. J. Nucl. Phys.* **42**, 712 (1985).

[6] A.S. Botvina *et al.*, *Nucl. Phys.* **A475**, 663 (1987).

[7] A.S. Botvina, A.S. Iljinov, I.N. Mishustin, *Nucl. Phys.* **A507**, 649 (1990).

[8] J.P. Bondorf *et al.*, *Phys. Rep.* **257**, 133 (1995).

[9] A. Kelić, M.V. Ricciardi, K.-H. Schmidt, Proceedings of the Joint ICTP-IAEA Advanced Workshop on Model Codes for Spallation Reactions, ICTP Trieste, Italy, 4–8 February 2008, D. Filges *et al.*, Eds., IAEA INDC(NDS)-530, Vienna, 2008, p. 181, available from: `http://www-nds.iaea.org/reports-new/indc-reports/indc-nds/indc-nds-0530.pdf` and `arXiv:0906.4193 [nucl-th]`.

[10] R.J. Charity *et al.*, *Nucl. Phys.* **A483**, 371 (1988).

[11] R.J. Charity, *Phys. Rev.* **C82**, 014610 (2010).

[12] S. Leray *et al.*, *Nucl. Instrum. Methods Phys. Res., Sect. B* **268**, 581 (2010).

[13] A. Boudard *et al.*, *Phys. Rev.* **C87**, 014606 (2013).

[14] S. Furihata, *Nucl. Instrum. Methods Phys. Res., Sect. B* **171**, 251 (2000).

[15] S. Furihata, T. Nakamura, *J. Nucl. Sci. Technol. Suppl.* **2**, 758 (2002).

[16] K. Kwiatkowski *et al.*, *Phys. Rev. Lett.* **50**, 1648 (1983).

[17] M.S. Sabra *et al.*, *Nucl. Instrum. Methods Phys. Res., Sect. B* **269**, 2463 (2011).

[18] G. Folger, V.N. Ivanchenko, J.P. Wellisch, *Eur. Phys. J.* **A21**, 407 (2004).

[19] M.I. Baznat, K.K. Gudima, S.G. Mashnik, A.J. Sierk, Vienna Meeting on Intercomparison of Spallation Reaction Models, IAEA, Vienna, Austria, 4–8 May, 2009.

[20] K. Niita *et al.*, *Phys. Rev.* **C52**, 2620 (1995).

[21] K. Niita *et al.*, *Radiat. Meas.* **41**, 1080 (2006).

[22] B. Compani-Tabrizi, F.B. Malik, *J. Phys. G* **8**, 1447 (1982).

[23] M.S. Sabra, Z.F. Shehadeh, F.B. Malik, *Eur. Phys. J.* **A27**, 167 (2006).

[24] R. Silberberg, C.H. Tsao, *Astrophys. J.* **25**, 315 (1973).

[25] A.Yu. Konobeyev *et al.*, *J. Korean Phys. Soc.* **59**, 927 (2011).

[26] S.K. Sharma, *Acta Phys. Pol. Proc. Suppl. B* **6**, 1161 (2013).